Maxillary Sinus Augmentation without Grafting Material with Simultaneous Implant Installation: A Three-Dimensional Finite Element Analysis

Xu Yan, DDS, SMD;[§] Xinwen Zhang, DDS, PhD;[*] Jie Gao, DDS, PhD;[†] Yasuyuki Matsushita, DDS, PhD;[†] Kiyoshi Koyano, DDS, PhD;[†] Xi Jiang, DDS, SMD;[‡] Hongjun Ai, DDS, PhD[§]

ABSTRACT

Purpose: The study aims to provide a theoretical guidance of postmaxillary implant in the augmented sinus without grafting materials by establishing a three-dimensional model of this new implant restorative technique, evaluating failure risk of sinus augmentation without grafting materials of different alveolar ridge heights, and analyzing stress distribution of different healing stage.

Materials and Methods: Seventeen three-dimensional finite element models of a posterior maxillary region with sinus mucosa and different elevation heights were constructed according to anatomical data of sinus area, and the standard implant model based on Nobel Biocare implant system were created via computer-aided design software. All materials were assumed to be isotropic and linearly elastic. Axial force of 150 N was applied. The von Mises stress, stress distribution, and implant displacement were calculated with software.

Results: With the height of the alveolar ridge reducing, the maximum von Mises stress of tissues and the displacement of the implant are on the rise, especially when the height of the bone is less than 7 mm. When the height decreased to 4 mm, the data may be doubled. After the stiff callus stage, the stress and displacement were close to the control model.

Conclusion: For maxillary sinus augmentation without grafting material implant technique, the stress of different tissues and the displacement of the implant were not increased much when the height of alveolar ridge is more than 7 mm. But if the alveolar bone height is less than 4 mm, this implant technique is not suggested. Immediately loading is not suggested and the loading opportunity should be after the stiff callus stage at least to improve the success rate.

KEY WORDS: dental implants, finite element analysis, maxillary sinus augmentation without grafting material, stress distribution

INTRODUCTION

Implant restoration of lost dentition in posterior maxilla is limited by the reducing height of residual vertical alveolar bone. Elevation of the sinus membrane with subsequent augmentation of sinus bone graft is clinically proven to be a safe technique in the past few decades.[1] Various types of modified surgical methods have been proposed to improve the efficacy of the treatment with smaller injuries, shorter operation time and less complications.[1–3] Moreover, a variety of graft materials has been developed to get better primary stability and higher success rate of the implant in the concept that implants should be completely wrapped by bone or bone graft material.[4–7]

Recently, the relevance of placing a grafting material in sinus elevation procedures has been questioned.[8–11] It has been reported that, according to the principles of guided bone regeneration, membrane elevation with space maintenance and blood clot formation might be sufficient to obtain bone formation in this newly created space.[12] Palma and colleagues[12] reported that the

*Center of Implant Dentistry, School of Stomatology, China Medical University, Shenyang, China; †Section of Removable Prosthodontics, Division of Oral Rehabilitation, Faculty of Dental Science, Kyushu University, Fukuoka, Japan; ‡Department of Oral Implantology, School and Hospital of Stomatology, Peking University, Beijing, China; §Department of Prosthodontics, School of Stomatology, China Medical University, Shenyang, China

Corresponding Author: Dr. Xu Yan, Department of Prosthodontics, School of Stomatology, China Medical University, No.117 Nanjing North Street, Heping District, Shenyang 110001, China; e-mail: xuyan5119@yeah.net

DOI 10.1111/cid.12254

amount of augmented bone tissue in the maxillary sinus after sinus membrane elevation with or without adjunctive autogenously bone grafts had no difference after 6 months of healing. And the sinus membrane showed good osteoinductive potential. Nedir and colleagues[11] treated 17 patients who presented an average residual bone height of 5.4 mm and placed 25 implants protruding in the sinus without introduction of a grafting material. A healing period of 3 to 4 months was allowed before abutment tightening at 35 Ncm. All implants achieved osseointegration and were stable after 1 year of loading. The authors reported that all implants gained 2.5 ± 1.2 mm endo-sinus bone in average. However, all the studies about sinus floor augmentation without bone graft are animal experiments.

In the past three decades, finite element analysis (FEA) has been used extensively to predict the biomechanical performance of various clinical factors on the success of implantation.[13] The distribution of forces in peri-implant bone of sinus area has been investigated by three-dimensional FEA in several studies,[14–16] but none of this concerns sinus floor augmentation without bone graft. Sinus membrane trauma or exceeding micro motion occurs easily in the preliminary stage of sinus floor elevation with simultaneous implant installation because of the poor osseointegration between implant and bone[17] which may lead to early failures. Recently, to simulate this early contact relationship between implant and bone, Ding and colleagues have reported a new three-dimensional finite element method to analyze stress distribution of immediate loading implant by using nonlinear frictional contact elements, which allows minor displacements between implant and bone.[18]

The aim of this study was to provide a theoretical guidance of postmaxillary implant in the augmented sinus without grafting materials by establishing a three-dimensional model of this new implant restorative technique, evaluating the failure risk of sinus augmentation without grafting materials of different alveolar ridge heights, and analyzing stress distribution of different healing stage.

MATERIALS AND METHODS

Sinus Geometric Modeling

Three-dimensional CAD models of posterior maxilla with 0.3 mm thick[19] sinus membrane, different heights of atrophic alveolar ridge, and different elevation heights were generated using computer-aided design software (SolidWorks 2012, Fukuoka, Japan). The geometry of the maxilla was defined by a bucco-palatal section according to the anatomical aspects of sinus area.[20–23] The elevation heights were described by different height level of sinus membrane. The total heights of the native bone component were from 2 mm to 10 mm, consisting of 1-mm crestal cortical bone, 0.5-mm sinus floor cortical bone, and 0.5-mm to 8.5-mm cancellous bone. Nine models (Model 1-1 to 1-9) of different heights of the alveolar ridges, whose native bone height and elevated height was 10 mm in total, were researched for the different alveolar ridge heights and sinus elevation heights. The heights of the alveolar ridges of Model 1-2 to Model 1-9 were from 9 mm to 2 mm. The model 1-1 was the control model, of which alveolar ridge height was 10 mm without sinus elevated. Seven of the other eight models (Model 2-1 to 2-7) with the alveolar ridge of 7-mm height were for the research of different healing stage of sinus floor elevation without bone graft with simultaneous implant installation. The basic overall geometry of the sinus area is identical for these seven models. Tissue differentiation and gradual stiffening of the callus tissue are the fundamental processes of healing. These processes were simulated by changing the element material properties from one stage to the next. Furthermore, a control model (Model 2-8) was established to describe sinus floor elevation with bone graft with conventional loading. The characterization of the histomorphological sequence of the healing process and the types of tissue involved were listed in Table 1.

Implant System

The standard implant with a diameter of 4.0 mm and a length of 10.0 mm was modeled (the shape and structure was according to Nobel Biocare implant system) and placed in the three-dimensional finite element models of membrane-elevated sinus. To simplify the analysis, the model of the implant and the abutment was modeled as a unit.

Material Properties

The material properties of different kinds of tissues, as well as implants in the models were assumed to be homogeneous, isotropic, and linearly elastic. Young's modulus and Poisson's ratio of materials used in the analysis were taken from the literature,[18,24–26] as shown in Table 2.

TABLE 1 Study Models for Different Healing Stages

Model No.	Model 2-1	Model 2-2	Model 2-3	Model 2-4	Model 2-5	Model 2-6	Model 2-7	Model 2-8 (Control)
Loading opportunity	Within 48 hours Immediate loading		4 weeks	Early loading	8 weeks		3–6 months Conventional loading	3–6 months Conventional loading
Healing stage	Initial blood and granulation tissue	Between initial blood and soft callus	Soft callus	Between soft callus and stiff callus	Stiff callus	Between stiff callus and chondroid ossification	Chondroid ossification	Bone graft

TABLE 2 Material Properties Ascribed to Materials Used in the Models

Material	Young's Modulus (MPa)	Poisson's Ratio
Titanium implant[19]	103,400	0.35
Cortical bone[19]	13,700	0.3
Cancellous bone (D3)[19]	1,370	0.3
Initial blood and granulation tissue[25]	1	0.17
Between initial blood and soft callus	500	0.3
Soft callus[26]	1,000	0.3
Between soft callus and stiff callus	3,500	0.3
Stiff callus[26]	6,000	0.3
Between stiff callus and chondroid ossification	8,000	0.3
Chondroid ossification[26]	10,000	0.3
Bone graft[27]	11,000	0.3
Sinus membrane[20]	58	0.45

Interface Conditions

Model 2-7 and Model 2-8 were presumed to represent ideal osseointegration, with 100% union between the newly formed bone, implants, bone graft, and maxilla. For Model 2-1 to 2-6 and Model 1-1 to 1-9, the implant–bone interface was assumed as a frictional interface (before osseous integration). To obtain initial stability for the situation of immediate loading after implantation, it was modeled using nonlinear frictional contact elements, which allowed minor displacements between implant and bone. Under these conditions, the contact zone transfers pressure and tangential forces (i.e., friction), but no tension. The friction coefficient was set to 0.3 between implant and bone/callus; and 0.05 between implant and initial blood and granulation tissue.[27,28]

Loading and Boundary Conditions

An average occlusal force of 150 N[29] was vertical loaded dispersedly on the top of the implant abutment. Ansys FE software (Solidworks 2012) was used for FEA. All models were constrained in all directions at the nodes on the mesial and distal bone surfaces, the top of the simulated sinus, sinus walls, and sinus membrane. These models were meshed with 8-nodes-tetrahedral elements and composed of elements varying from 73,638 to 100,085, and nodes ranging from 116,806 to 157,898. The von Mises stress values were measured in all kinds of the implant surrounding tissues along the tissue-implant interface. To assess the distribution of stresses, von Mises stresses were visualized with stress contour plots. The biomechanical effects were also analyzed by comparing the maximum displacement of the implant neck.

RESULTS

Different Alveolar Ridge Heights

Stress Distribution and Maximum von Mises stress

Cortical Bone. With the reduction of the height of the alveolar ridge, the highest stress the cortical bone suffered was on the rise. Correspondingly, more stress was gathered in crestal cortical bone and sinus floor cortical bone, and was dispersed over smaller areas of the inner and outer sinus walls. However, not all the highest stress was concentrated around the implant neck. For Model 1-5 to Model 1-9 and Model 1-1 (Control), the highest stress was around the implant neck, but for Model 1-2 to Model 1-4, the highest stress concentrated on the sinus floor cortical bone around the implant.

The maximum von Mises stress on crestal cortical bone was slowly increasing by about 3.5 MPa from 22.9 MPa to 32.8 MPa, with the alveolar ridge decreased from 9 mm to 6 mm. With the alveolar ridge decreasing from 6 mm to 2 mm, there were two rapid increasing stages of the maximum von Mises stress. In the first stage, the height of alveolar ridge decreased from 6 mm to 4 mm, while the stress increased by 6 MPa. When the

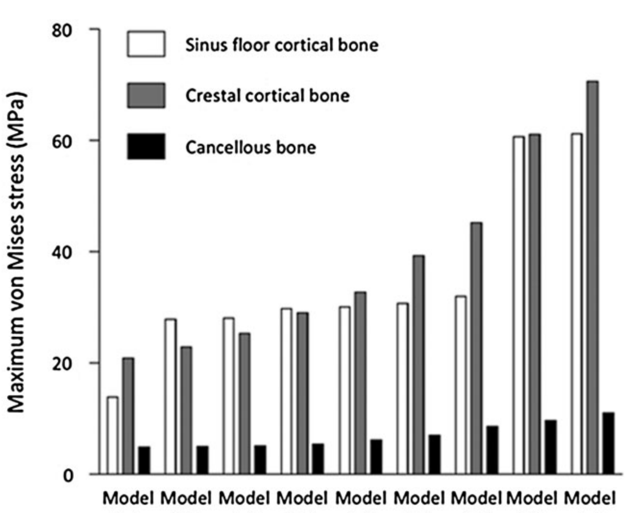

Figure 1 Maximum von Mises stress in sinus floor cortical bone, crestal cortical bone, and cancellous bone of Model 1-1 to Model 1-9.

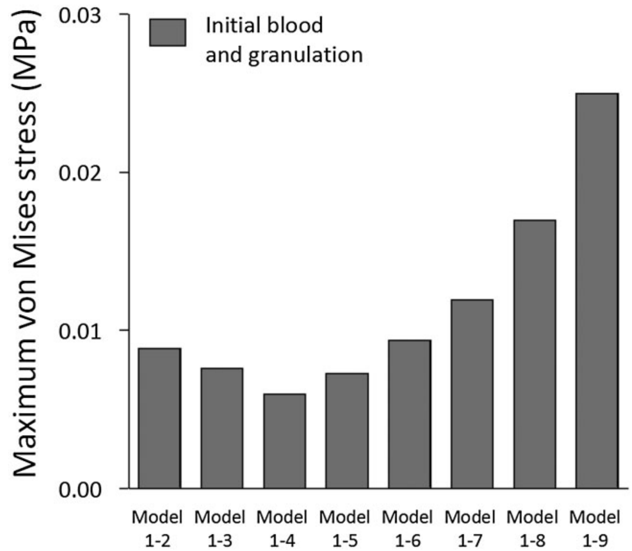

Figure 2 Maximum von Mises stress in initial blood and granulation tissue of Model 1-2 to Model 1-9.

height of the alveolar ridge was less than 4 mm, the maximum von Mises stress increased with a faster rate. In contrast, the maximum von Mises stress in sinus floor cortical bone remained in the same level of about 30 MPa until the height of the alveolar ridge decreased to 4 mm. After that, the stress rapidly doubled (Figure 1).

Cancellous Bone. It was the same with the cortical bone; the more the height of the alveolar ridge was reduced, the more the highest stress the cancellous bone was suffered. When the height of the alveolar ridge was less than 7 mm, the stress increased faster (see Figure 1). Cancellous bone around the tips and the upper surfaces of the threads suffered more stress.

Initial Blood and Granulation Tissue. Although the maximum von Mises stress was very low, the trend of different heights of the alveolar ridges was much different. The highest stress decreased with the reduction of the alveolar bone from 9 mm to 7 mm, and then increased with a much higher increasing rate with the continued reduction of the alveolar bone (Figure 2). The same with cancellous bone, the highest stress was mainly around the tips and the upper surfaces of the threads.

Sinus Membrane. The maximum von Mises stress increased with the reduction of the height of the alveolar ridge. The increasing trend became faster when the height of the alveolar ridge was less than 5 mm

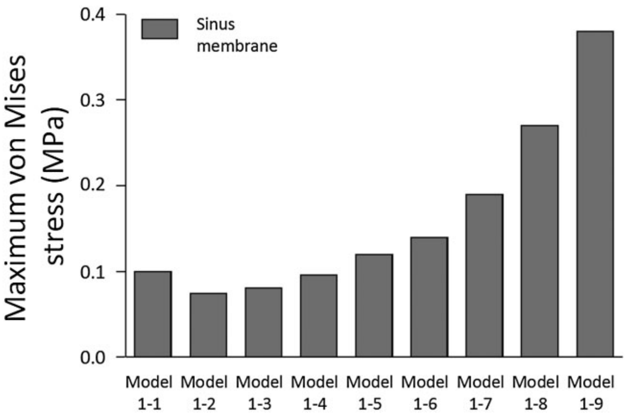

Figure 3 Maximum von Mises stress in sinus membrane of Model 1-1 to Model 1-9.

(Figure 3). Figure 3 also showed that, with the buffer of little amount of blood, the maximum von Mises stress of Model 1-2 and Model 1-3 was even less than Model 1-1 (control), and Model 1-4 got the same level with Model 1-1 (control). Figure 4 showed that the maximum von Mises stress was not in the center of the raised membrane jacked up by the implant, but in the turning area around the raised membrane.

Implant Displacement. Compared with the control Model (Model 1-1), the reduction of the alveolar ridge height affect the displacements of the implant. The maximum displacement of implant increased, with the decreasing of the height of the alveolar ridge. The maximum displacement was not higher than 5% compared with Model 1-1, until the height decreased to 7 mm (Model 1-4). When the alveolar bone height decreased to 4 mm, maximal displacement of the implant increased considerably (see Figure 4). For each certain model, minor movement of the implant as a whole was allowed and the displacement of an implant was almost the same, except for that which was wider between abutment and the neck (Figure 5).

Different Healing Stages

As the blood filled in the elevation space of the sinus, the maximum von Mises stress upon cortical bone and cancellous bone reduced gradually (Figure 6). Compared with Model 2-8, the maximum von Mises stresses upon cortical bone and cancellous bone were 188% and 164% in the initial blood stage (Model 2-1), while the stress decreased to 113% and 106% in the stiff callus stage (Model 2-5). Figure 6 also showed that this reduction was slowing down after "Stiff callus stage." As the callus became harder, the von Mises stress appeared beeline ascending (Figure 7), which decreased the area of thrust surface in alveolar cortical bone and sinus floor cortical bone, and also made the stress of the implant spread to the top and more evenly. The maximum von Mises stress upon sinus membrane of Model 2-1 (blood stage) and Model 2-7 (Chondroid ossification stage) was more or less the same with Model 2-8 (control). Once the blood clotted, the maximum von Mises stress of sinus membrane was significantly increased to 216% compared with the control model. After that, the stress upon sinus membrane declined gradually (Figure 8). Implant displacements also showed a decreasing trend with the organization of the blood. In blood stage (Model 2-1), the maximum displacement was 138% compared with the control model, and decreased to 107% at the stiff callus stage (Figure 9).

DISCUSSION

Model

The sinus area of posterior maxilla is so complex that it is not easy to get an accurate three-dimensional model. Okumura and colleagues reported that there were no much difference between conventional simplified three-dimensional finite element models and the full maxilla model created from CT DICOM data in the FEM research of maxilla sinus area implant.[30] To exclude the influences of anatomical variations of bone and ensure the comparability of the models as suggested by Akca and Cehreli,[31] we decided not to use an anatomical model of maxilla provided by Cone Beam Computed

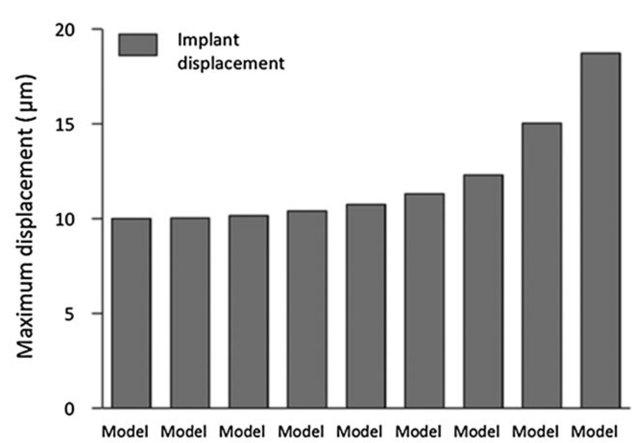

Figure 4 Maximum displacement of the implant neck of Model 1-1 to Model 1-9.

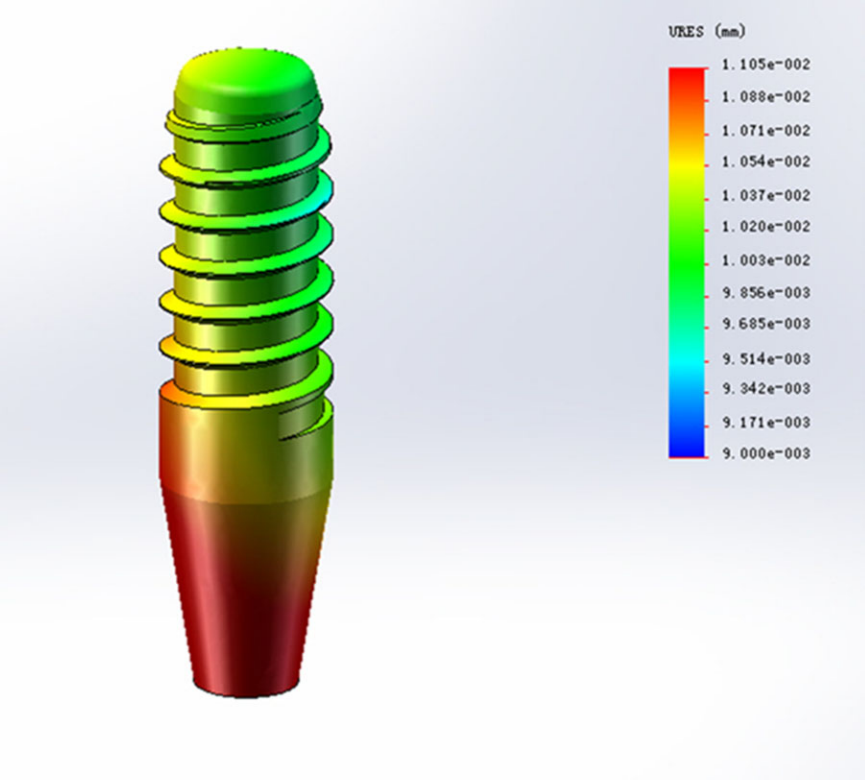

Figure 5 A typical example (Model 1-4) of the displacement of the implant.

Tomography (CBCT) data, but rather three-dimensional CAD models based on the same sketch which were developed according to the anatomic data of sinus area. The height of sinus floor was considered to be stable in long term.[32] Therefore, we developed alveolar bone models by reducing the height of alveolar ridges and keep the sinus floor and other upper structure stable to better simulate atrophy alveolar ridge and make the models more comparable. Furthermore, we build the models of blood clot and sinus membrane, as well as friction coefficient between the implant and bone/blood clot. We evaluated the range of application on longitudinal variation of the alveolar ridge heights and also the lateral variation of different healing stages.

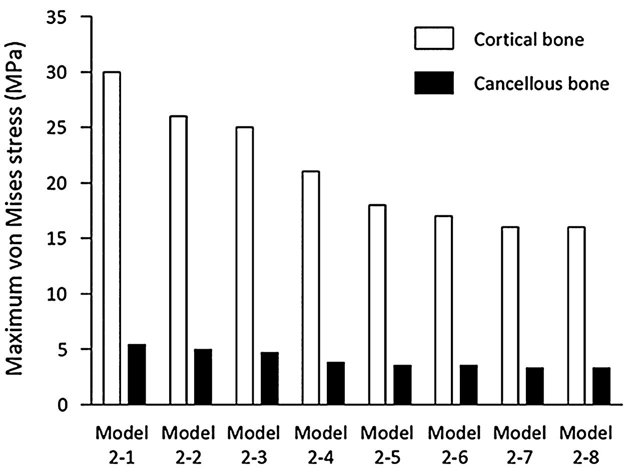

Figure 6 Maximum von Mises stress in cortical bone and cancellous bone of Model 2-1 to Model 2-8.

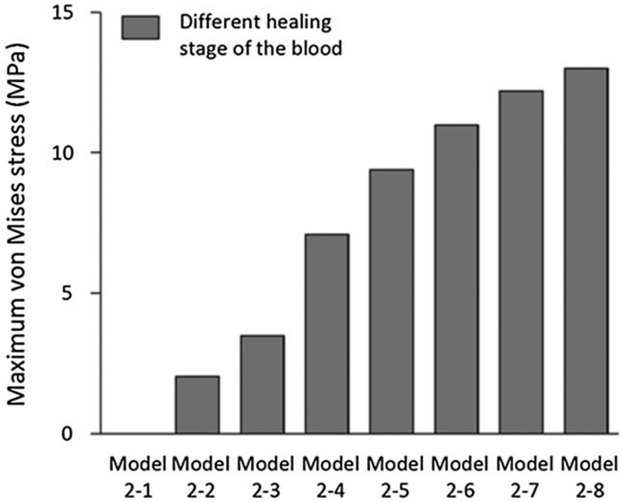

Figure 7 Maximum von Mises stress in different healing stage of the blood of Model 2-1 to Model 2-8.

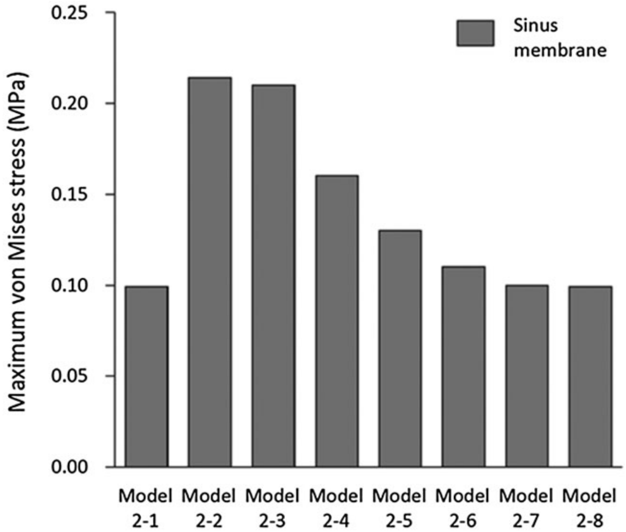

Figure 8 Maximum von Mises stress in sinus membrane of Model 2-1 to Model 2-8.

Different Alveolar Ridge Heights

The residue alveolar ridge height has been already proven to be a critical factor of implant by many clinical studies.[21,33,34] To solve the problem of insufficient vertical alveolar bone, sinus elevation with autogenous bone or bone substitute materials were used and already achieved good treatment effectiveness.[33–35] Although Thor and colleagues[36] and Gabbert and colleagues[17] have reported successful clinical application of sinus lift without graft material, there are still only a few dentists who trust this implant treatment for they worry of complications such as membrane perforation and early failure. There are already a few FEM studies about sinus lift with bone graft. For example, Huang and colleagues[37] and Inglam and colleagues[38] reported that bone graft stiffness affect the stress distribution. But still, there are few theoretical studies about sinus augmentation without grafting material with simultaneous implant installation.

From the result of our study, the stress on blood was the lowest when the alveolar ridge height was 7 mm, which means that the influence of the stress was least to the blood. Compared to the stress distributed on the bones, few stress was on blood in all the models, which can hardly provide retention force to the implant. Fanuscu and colleagues[39] reported that the crestal cortical bone received the highest intensity stresses in grafted sinus model with the alveolar ridge of 5 mm. In agreement with a previous study,[40] cortical bone is the main part to fasten the implant. However, in our research, when the height of the residual alveolar ridge was more than 7 mm, the highest stress was not in the crestal cortical but in the sinus floor cortical bone, which meant that sinus floor cortical bone might play an important role in stress distribution. On one hand, if the stress concentrates too much on the sinus floor, fractures can happen after loading; on the other hand, the thick and high-intensive sinus floor may reduce the stress on crestal cortical bone to relieve the marginal bone loss in sinus lift. The result of our study indicated that the stress and displacement did not increase much when the height of the alveolar ridge was more than 7 mm, which coincided with the clinical findings of osteogenesis.[12] But when the alveolar bone height was less than 4 mm, the stress and displacement might be doubled, which suggested that failure might happen.

Sinus mucosa perforation is one of the most important complications of sinus elevation. It has been already shown that the sinus mucosa remains healthy after maxillary sinus floor elevation using a grafting material.[41,42] Sul and colleagues[43] evaluated the histologic changes in the maxillary sinus membrane after sinus lift and simultaneous insertion of implants without additional grafting material. They reported that sinus membrane wrapped the top of the implant compactly and little influence was found on the histologic characteristics of the sinus membrane. Some other clinical studies[2,36] also indicated that sinus lift without bone grafting material can not only make the top of the implant and sinus membrane form a firm contact relation without any clinical symptoms, but also had the effect of

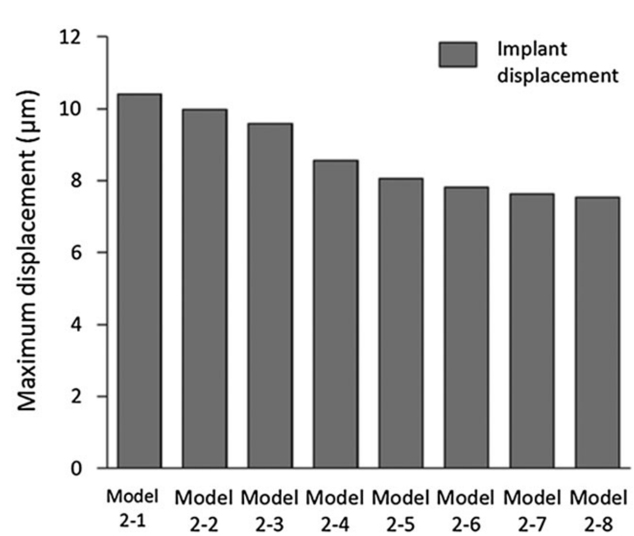

Figure 9 Maximum displacement of the implant neck of Model 2-1 to Model 2-8.

osteoinduction and bone augmentation. In our study, because of the buffer of the blood, the stress on sinus membrane was even lower than the control model when the height of residual alveolar ridge was more than 7 mm. Otherwise, the stress presented a trend of rapid rising and nearly doubled when the alveolar ridge height reduced to 4 mm. Similar with the result of stress distribution, this result showed that 7 mm and 4 mm were the safe and risky indicators. Liu and colleagues' study[44] has shown that the biggest stress was in the center of the raised membrane. However, the stress distribution of sinus membrane was shown in the turning area around the raised membrane in our study. The difference might be due to the design of the top of the implant. In our study, the top of implant was designed to be flat preventing stress converged on one point. The result of stress distribution also suggested that lessening the tension of the membrane was of great importance to prevent sinus membrane trauma.

Different Healing Stages

The loading opportunity of the implant is a topic of much debate. Although for sinus floor elevation with grafting material, some researchers have already made proposals for the loading opportunity.[45] There is no universal agreement on the loading opportunity of sinus lift without grafting material. In our study, the models of different healing stages were also the simulation of different loading times. As for the assembling of the blood, the maximum von Mises stress on cortical bone and cancellous bone was decreased. After the stage of "stiff callus", the decrease slowed down. For the stage of initial blood, the maximum von Mises stresses on cortical bone and cancellous bone were 188% and 164%, while at the stiff callus stage, the stress dropped to 113% and 106%, respectively. With the organization of the blood, it becomes harder and harder, which makes it capable of withstanding more forces. The stress and stress distribution area decreased, and the stress on the implant dispersed from the abutment and implant neck to the whole implant. The stress on sinus membrane reached the peak of 216% in soft callus stage compared with control model, and then slowly decreased. It is very dangerous to load early for the excessive force acting on sinus membrane. Implant displacement continuously decreased with the organization of the blood and dropped to 107% compared with the control model. After the stiff callus stage, the decrease of the implant displacement slowed down. Thus, during the course of blood organization, the loading time should be postponed to stiff callus stage at least, which means 2 months after simultaneous implant installation.

CONCLUSION

With the decrease of alveolar ridge height, the stress on different tissues and the displacement of the implant increased correspondingly, which might raise the risk of overloaded bone loss and poor primary stability. The stress and displacement did not increase much when the height of alveolar ridge was more than 7 mm, which coincided with the clinical finding of osteogenesis. However, when the alveolar bone height was less than 4 mm, the stress and displacement might be doubled, which suggested that failure of implantation could happen. Immediate loading was not recommended, and the loading opportunity should be after the stiff callus stage to improve the success rate.

ACKNOWLEDGMENTS

This research was supported by School of Stomatology, China Medical University, Shenyang, China (grantsK101593-12-34). The authors would like to thank the Regenerative Dentistry and Implant Center, and Section of Removable Prosthodontics, Division of Oral Rehabilitation, the Faculty of Dental Science, Kyushu University, Fukuoka, Japan, for their support and allowing us to use of their facilities.

REFERENCES

1. Del Fabbro M, Testori T, Francetti L, et al. Systematic review of survival rates for implants placed in the grafted maxillary sinus. J Periodontics Restorative Dent 2004; Dec; 24(6):565–577.
2. Lundgren S, Anderson S, Gualini F, et al. Bone reformation with sinus membrane elevation: a new surgical technique for maxillary sinus floor augmentation. Clin Implant Dent Relat Res 2004; 6:165–173.
3. Zijderveld SA, Zerbo IR, Van Den Bergh JP, et al. Maxillary sinus floor augmentation using a beta-tricalcium phosphate (Cerasorb) alone compared to autogenous bone grafts. Int J Oral Maxillofac Implants 2005; 20:432–440.
4. Wetzel AC, Stich H, Caffesse RG. Bone apposition onto oral implants in the sinus area filled with different grafting materials. A histological study in beagle dogs. Clin Oral Implants Res 1995; 6:155–163.
5. Hürzeler MB, Quiñones CR, Kirsch A, et al. Maxillary sinus augmentation using different grafting materials and dental

implants in monkeys. Clin Oral Implants Res 1997; 8:476–486.

6. Doi K, Oue H, Morita K, et al. Development of implant/interconnected porous hydroxyapatite complex as new concept graft material. PLoS ONE 2012; 7:e49051.
7. Mertens C, Wiens D, Steveling HG, et al. Maxillary sinus-floor elevation with nanoporous biphasic bone graft material for early implant placement. Clin Implant Dent Relat Res 2012; 5. doi: 10.1111/j.1708-8208.2012.00484.x. [Epub ahead of print]
8. Winter AA, Pollack AS, Odrich RB. Placement of implants in the severely atrophic posterior maxilla using localized management of the sinus floor: a preliminary study. Int J Oral Maxillofac Implants 2002; 17:687–695.
9. Winter AA, Pollack AS, Odrich RB. Sinus/alveolar crest tenting (SACT): a new technique for implant placement in atrophic maxillary ridges without bone grafts or membranes. Int J Periodontics Restorative Dent 2003; 23:557–565.
10. Lundgren S, Andersson S, Sennerby L. Spontaneous bone formation in the maxillary sinus after removal of a cyst: coincidence or consequence?. Clin Implant Dent Relat Res 2003; 5:78–81.
11. Nedir R, Bischof M, Vazquez L, et al. Osteotome sinus floor elevation without grafting material: a 1-year prospective pilot study with ITI implants. Clin Oral Implants Res 2006; 17:679–686.
12. Palma VC, Magro-Filho O, Oliveria D, et al. Bone reformation and implant integration following maxillary sinus membrane elevation: an experimental study in primates. Clin Implant Dent Relat Res 2006; 8:11–24.
13. Van Staden RC, Guan H, Loo YC. Application of the finite element method in dental implant research. Comput Methods Biomech Biomed Engin 2006; 9:257–270.
14. Li T, Yang X, Zhang D, et al. Analysis of the biomechanical feasibility of a wide implant in moderately atrophic maxillary sinus region with finite element method. Oral Surg Oral Med Oral Pathol Oral Radiol 2012; 114:e1–e8.
15. Schuller-Götzburg P, Entacher K, Petutschnigg A, et al. Sinus elevation with a cortical bone graft block: a patient-specific three-dimensional finite element study. Int J Oral Maxillofac Implants 2012; 27:359–368.
16. Okumura N, Stegaroiu R, Kitamura E, et al. Influence of maxillary cortical bone thickness, implant design and implant diameter on stress around implants: a three-dimensional finite element analysis. J Prosthodont Res 2010; 54:133–142.
17. Gabbert O, Koob A, Schmitter M, Rammelsberg P. Implants placed in combination with internal sinus lift without graft material: an analysis of short-term failure. J Clin Periodontol 2009; 36:177–183.
18. Ding X, Zhu XH, Liao SH, et al. Implant–bone interface stress distribution in immediately loaded implants of different diameters: a three-dimensional finite element analysis. J Prosthodont 2009; 18:393–402.
19. Pommer B, Unger E, Sütö D, et al. Mechanical properties of the Schneiderian membrane in vitro. Clin Oral Implants Res 2009; 20:633–637.
20. Underwood AS. An inquiry into the anatomy and pathology of the maxillary sinus. J Anat Physiol 1910; 44(Pt 4):354–369.
21. Ulm CW, Solar P, Gselimann B, et al. The edentulous maxillary alveolar process in the region of the maxillary sinus – a study of physical dimension. Int J Oral Maxillofac Surg 1995; 24:279–282.
22. Bergh J, Bruggenkate CM, Disch FJM, et al. Anatomical aspects of sinus floor elevations. Clin Oral Implants Res 2000; 11:256–265.
23. Gosau M, Rink D, Driemel O, et al. Maxillary sinus anatomy: a cadaveric study with clinical implications. Anat Rec 2009; 292:352–354.
24. Lacroix D, Prendergast PJ, Li G, et al. Biomechanical model to simulate tissue differentiation and bone regeneration: application to fracture healing. Med Biol Eng Comput 2002; 40:14–21.
25. Claes LE, Heigele CA. Magnitudes of local stress and strain along bony surfaces predict the course and type of fracture healing. J Biomech 1999; 32:255–266.
26. Rues S, Lenz J, Schierle HP, et al. Simulation of the sinus floor elevation. Proc Appl Math Mech 2004; 4:368–369.
27. Viceconti M, Monti L, Muccini R, et al. Even a thin layer of soft tissue may compromise the primary stability of cementless hip stems. Clin Biomech (Bristol, Avon) 2001; 16:765–775.
28. Mellal A, Wiskott HWA, Botsis J, et al. Stimulating effect of implant loading on surrounding bone. Clin Oral Implants Res 2004; 15:239–248.
29. Cattaneo PM, Dalstra M, Melsen B. The transfer of occlusal forces through the maxillary molars: a finite element study. Am J Orthod Dentofacial Orthop 2003; 123:367–373.
30. Okumura N, Stegaroiu R, Nishiyama H, et al. Finite element analysis of implant-embedded maxilla model from CT data: comparison with the conventional model. J Prosthodont Res 2011; 55:24–31.
31. Akca K, Cehreli MC. Biomechanical consequences of progressive marginal bone loss around oral implants: a finite element stress analysis. Med Biol Eng Comput 2006; 44:527–535.
32. Ariji Y, Ariji E, Yoshiura K, et al. Computed tomographic indices for maxillary sinus size in comparison with the sinus volume. Dentomaxillofac Radiol 1996; 25:19–24.
33. Block MS, Kent JN. Endosseous implants for maxillofacial reconstruction. Philadelphia: WB Saunders, 1995:696.
34. Ferrigno N, Laureti M, Fanali S. Dental implants placement in conjunction with osteotome sinus floor elevation: a

12-year life-table analysis from a prospective study on 588 ITI implants. Clin Oral Implants Res 2006; 17:194–205.
35. Del Fabbro M, Rosano G, Taschieri S. Implant survival rates after maxillary sinus augmentation. Eur J Oral Sci 2008; 116:497–506.
36. Thor A, Sennerby L, Hirsch JM, et al. Bone formation at the maxillary sinus floor following simultaneous elevation of the mucosal lining and implant installation without graft material: an evaluation of 20 patients treated with 44 Astra Tech implants. J Oral Maxillofac Surg 2007; 65:64–72.
37. Huang HL, Fuh LJ, Ko CC, et al. Biomechanical effects of a maxillary implant in the augmented sinus: a three-dimensional finite element analysis. Int J Oral Maxillofac Implants 2008; 24:455–462.
38. Inglam S, Suebnukarn S, Tharanon W, et al. Influence of graft quality and marginal bone loss on implants placed in maxillary grafted sinus: a finite element study. Med Biol Eng Comput 2010; 48:681–689.
39. Fanuscu MI, Vu HV, Poncelet B. Implant biomechanics in grafted sinus: a finite element analysis. J Oral Implantol 2004; 30:59–68.
40. Koca OL, Eskitascioglu G, Usumez A. Three-dimensional finite-element analysis of functional stresses in different bone locations produced by implants placed in the maxillary posterior region of the sinus floor. J Prosthet Dent 2005; 93:38–44.
41. Bravetti P, Membre H, Marchal L, et al. Histologic changes in the sinus membrane after maxillary sinus augmentation in goats. J Oral Maxillofac Surg 1998; 56:1170–1176.
42. Timmenga NM, Raghoebar GM, Liem RSB, et al. Effects of maxillary sinus floor elevation surgery on maxillary sinus physiology. Eur J Oral Sci 2003; 111:189–197.
43. Sul SH, Choi BH, Li J, et al. Histologic changes in the maxillary sinus membrane after sinus membrane elevation and the simultaneous insertion of dental implants without the use of grafting materials. Oral Surg Oral Med Oral Pathol Oral Radiol Endod 2008; 105:e1–e5.
44. Liu XF, Hu LL, Song GB, et al. Effect of two different diameter implants on deformation of maxillary sinus mucosa: a three-dimensional finite element analysis. J Clin Rehabil Tissue Eng Res 2011; 15:9742–9745.
45. Esposito M, Grusovin MG, Achille H, et al. Interventions for replacing missing teeth: different times for loading dental implants. Cochrane Database Syst Rev 2013; 28;3:CD003878. doi: 10.1002/14651858.CD003878.pub5.